PNAS
www.pnas.org

Supporting Information for:

CHD7 and Runx1 interaction provides a braking mechanism for hematopoietic differentiation

Jingmei Hsu[1,2,14†], Hsuan-Ting Huang[3,14††], Chung-Tsai Lee[2], Avik Choudhuri[3], Nicola K. Wilson[4], Brian J. Abraham[5], Victoria Moignard[4], Iwo Kucinski[4], Shuqian Yu[2], R. Katherine Hyde[6†††], Joanna Tober[2], Xiongwei Cai[2], Yan Li[2], Yalin Guo[7], Song Yang[3], Michael Superdock[3], Eirini Trompouki[3††††], Fernando J. Calero-Nieto[4], Alireza Ghamari[8], Jing Jiang[9], Peng Gao[10], Long Gao[10], Vy Nguyen[3], Anne L. Robertson[3], Ellen M. Durand[3], Katie L. Kathrein[3], Iannis Aifantis[11], Scott A. Gerber[12], Wei Tong[9], Kai Tan[10,13], Alan B. Cantor[8], Yi Zhou[3], P. Paul Liu[6], Richard A. Young[5], Berthold Göttgens[4], Nancy A. Speck[2*], and Leonard I. Zon[3*]

Corresponding authors

Nancy A. Speck and Leonard Zon

Email: nancyas@upenn.edu and zon@enders.tch.harvard.edu

www.pnas.org/cgi/doi/10.1073/pnas.2003228117

This PDF file includes:

Figures S1 to S5

Table S1

List of Datasets S1 to S5

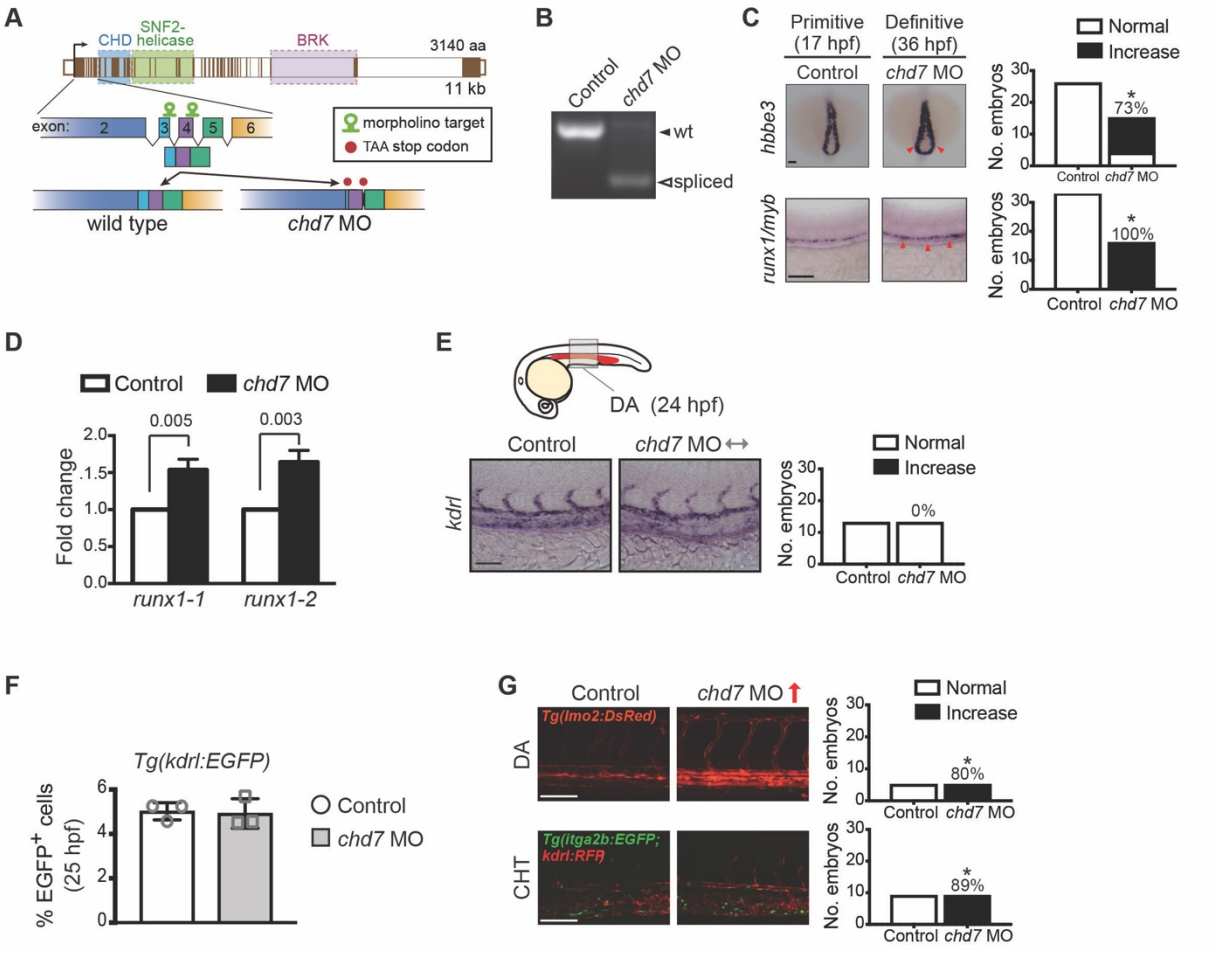
A
SNF2-
CHD helicase
BRK
3140 aa
11 kb
exon: 2 3 4 5 6
morpholino target
TAA stop codon
wild type
chd7 MO
B
Control
chd7 MO
wt
spliced
C
Primitive (17 hpf)
Definitive (36 hpf)
Control
chd7 MO
hbbe3
runx1/myb
Normal
Increase
No. embryos
73%
100%
Control chd7 MO
D
Control
chd7 MO
0.005
0.003
Fold change
runx1-1
runx1-2
E
DA (24 hpf)
Control
chd7 MO ↔
kdrl
Normal
Increase
0%
No. embryos
Control chd7 MO
F
Tg(kdrl:EGFP)
% EGFP+ cells (25 hpf)
Control
chd7 MO
G
Control
chd7 MO ↑
Tg(lmo2:DsRed)
Tg(itga2b:EGFP; kdrl:RFP)
DA
CHT
Normal
Increase
80%
89%
No. embryos
Control chd7 MO

Figure S1. *Chd7* knockdown and expression during zebrafish embryonic development. **A,** Schematic of zebrafish *chd7* gene and protein structure. *Chd7* splice blocking morpholinos (MO) targeting exons 3 and 4 introduce premature stop codons that eliminate all known conserved domains. Exons in solid fill and protein domains are marked with dotted lines. CHD, chromodomains. BRK, brahma and kismet domain. **B**, RT-PCR shows loss of wild-type (black arrowhead) transcript and appearance of *chd7* splice variant (white arrowhead) as a result of morpholinos targeting exons 3 and 4. **C**, Knockdown of *chd7* increases primitive erythroid *hbbe3* in the posterior lateral mesoderm and definitive HSPC *runx1* and *myb* expression in the dorsal aorta by whole mount *in situ* hybridization. Hpf, hours post-fertilization. Red arrowheads, increase. Phenotypic results of whole mount *in situ* hybridizations are quantified in bar graphs on the right. **p* < 0.01 by Chi-square test. Number of experiments = 2. **D**, Quantification of *runx1* expression in zebrafish embryos by qPCR with 2 sets of primers, normalized to *ef1α* (n=20-50 embryos), number of experiments= 5. **E,** Knockdown of *chd7* does not affect vascular *kdrl* expression by whole mount *in situ* hybridization. Blood flow was also not affected. Representative embryos are shown. Grey arrows, no change; n=2 experiments. **F**, Knockdown of *chd7* does not increase the number of vascular cells. Flow cytometric analysis of $EGFP^+$ cells from *Tg(kdrl:EGFP)* embryos at 25 hpf. Average of 3 independent experiments (n=14-90 embryos). Scale bars = 50 μm. **G**, Knockdown of *chd7* increases *lmo2* and *itga2b* expression in the dorsal aorta (DA) and caudal hematopoietic territory (CHT) in transgenic embryos. Images were acquired using the same confocal laser settings. Red arrow, increase. Results are quantified in bar graphs on the right. **p* < 0.01 by Chi-square test.

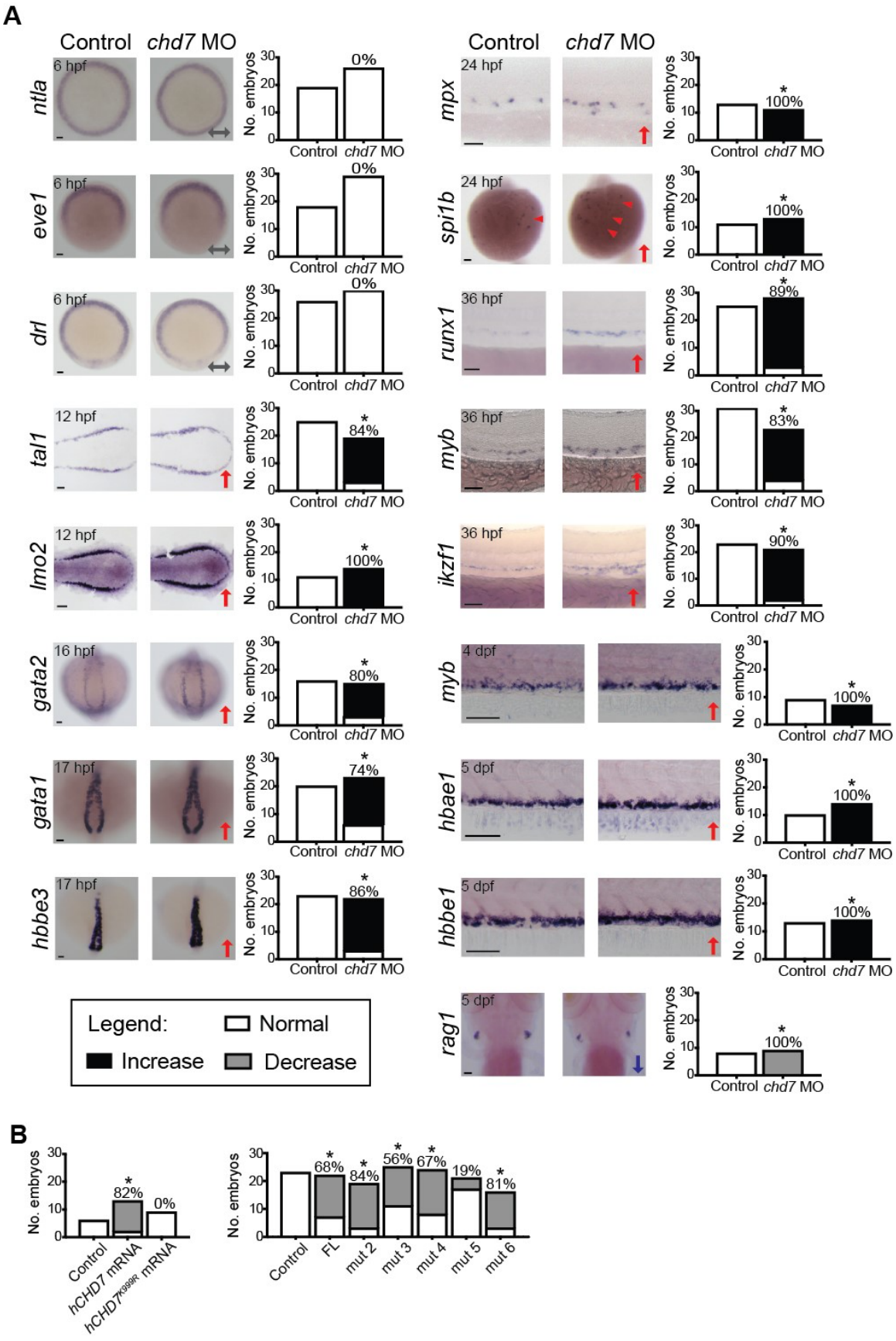
A
Control
chd7 MO
ntla
6 hpf
No. embryos
0%
Control
chd7 MO
eve1
6 hpf
0%
drl
6 hpf
0%
tal1
12 hpf
*
84%
lmo2
12 hpf
*
100%
gata2
16 hpf
*
80%
gata1
17 hpf
*
74%
hbbe3
17 hpf
*
86%
mpx
24 hpf
*
100%
spi1b
24 hpf
*
100%
runx1
36 hpf
*
89%
myb
36 hpf
*
83%
ikzf1
36 hpf
*
90%
myb
4 dpf
*
100%
hbae1
5 dpf
*
100%
hbbe1
5 dpf
*
100%
rag1
5 dpf
*
100%
Legend:
Normal
Increase
Decrease
B
No. embryos
*
82%
0%
Control
hCHD7 mRNA
hCHD7K999R mRNA
*
68%
*
84%
*
56%
*
67%
19%
*
81%
Control
FL
mut 2
mut 3
mut 4
mut 5
mut 6

Figure S2. Expression of multiple hematopoietic markers is elevated in chd7 morphant (MO) embryos. **A,** Representative whole mount *in situ* hybridization of chd7 morphant embryos for the genes listed in Figure 1A,B. Phenotypic results of whole mount *in situ* hybridizations are quantified in bar graphs (right). *$p < 0.01$ by Chi-square test. Red arrows and arrowheads, increase. Grey arrows, no change. Blue arrows, decrease. Scale bars = 50 μm; n= 2 experiments. **B,** Quantification of phenotypic results from Figure 4F,G. Same descriptions as in panel A.

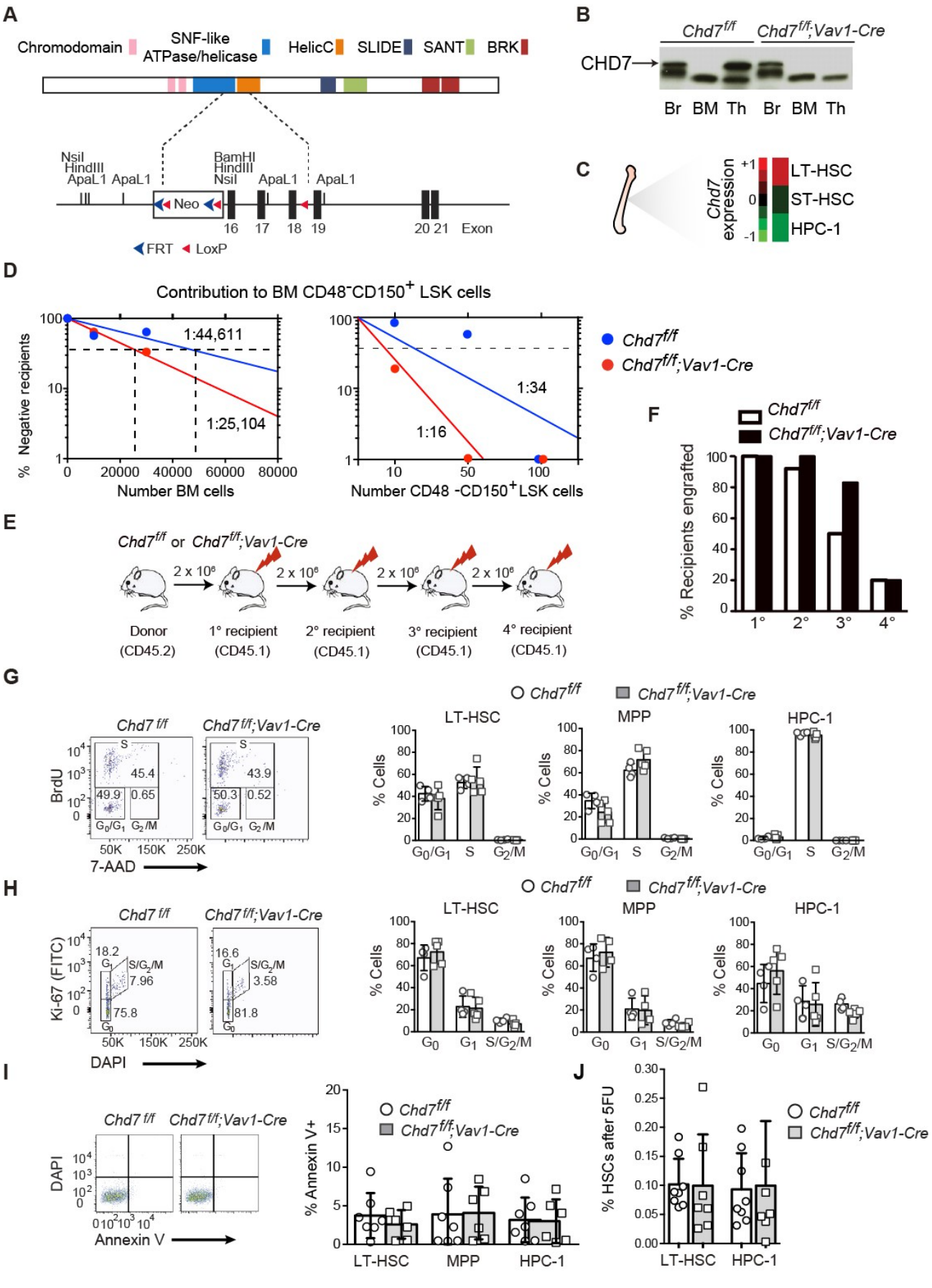
A
Chromodomain
SNF-like ATPase/helicase
HelicC
SLIDE
SANT
BRK
NsiI HindIII ApaL1 ApaL1
BamHI HindIII NsiI ApaL1 ApaL1
Neo
16 17 18 19
20 21 Exon
FRT LoxP
B
Chd7f/f
Chd7f/f;Vav1-Cre
CHD7
Br BM Th Br BM Th
C
Chd7 expression
+1
0
-1
LT-HSC
ST-HSC
HPC-1
D
Contribution to BM CD48-CD150+ LSK cells
% Negative recipients
1:44,611
1:25,104
Number BM cells
1:34
1:16
Number CD48 -CD150+LSK cells
Chd7f/f
Chd7f/f;Vav1-Cre
E
Chd7f/f or Chd7f/f;Vav1-Cre
2 x 10⁶
Donor (CD45.2)
1° recipient (CD45.1)
2° recipient (CD45.1)
3° recipient (CD45.1)
4° recipient (CD45.1)
F
Chd7f/f
Chd7f/f;Vav1-Cre
% Recipients engrafted
1° 2° 3° 4°
G
Chd7 f/f
Chd7 f/f;Vav1-Cre
BrdU
7-AAD
45.4
49.9
0.65
43.9
50.3
0.52
G0/G1 G2/M
LT-HSC
MPP
HPC-1
% Cells
G0/G1 S G2/M
H
Ki-67 (FITC)
DAPI
18.2
7.96
75.8
16.6
3.58
81.8
G0 G1 S/G2/M
I
Annexin V
% Annexin V+
LT-HSC MPP HPC-1
J
% HSCs after 5FU
LT-HSC HPC-1

Figure S3. Loss of *Chd7* in mice increases yolk sac, fetal liver, spleen, and bone marrow hematopoiesis. **A**, Schematic of the conditional mouse *Chd7* allele. Exons 16-18 were flanked by LoxP sites. The Neo gene was not deleted, but since *Chd7*$^{f/f}$ mice were grossly normal and did not exhibit the circling behavior characteristic of *Chd7* haploinsufficiency, expression from the allele is not significantly affected. **B**, Western blot showing absence of full length CHD7 protein (arrow) in the thymus (Th) of *Chd7*$^{f/f}$*;Vav1-Cre* mice. Brain (Br) tissue is the positive control. CHD7 is undetectable in whole bone marrow (BM). **C**, Expression of *Chd7* in sorted LT-HSC (CD48^{-} CD150^{+}CD34^{-}LSK), ST-HSC (CD48^{-}CD150^{+}CD34^{+}LSK), and HPC-1 (CD48^{+}CD150^{-}CD34^{+}LSK) populations from the mouse bone marrow analyzed on microarrays (MouseGene 2.0 ST arrays). *Chd7* mRNA is highest in LT-HSCs, and progressively decreases in ST-HSCs and HPC-1s. **D**, The frequency of functional CHD7 deficient LT-HSCs was not significantly increased in whole BM (left) and in purified CD48^{-}CD150^{+}LSK cells (right) when ≥1% donor contribution to CD48^{-} CD150^{+}CD34^{-}LSK cells in the BM was scored at 4 months. LT-HSC frequency was calculated by ELDA (n=7-14 recipients per dose). **E,** Schematic depicting serial transplantation of 2 x 10^{6} total bone marrow cells from *Chd7*$^{f/f}$ or *Chd7*$^{f/f}$*;Vav1-Cre* mice. **F**, CHD7 bone marrow cells have normal self-renewal measured by serial transplantation. The percent of engrafted mice is plotted (n=10 mice for each genotype). **G**, CHD7 deficiency does not affect proliferation of LT-HSCs, MPPs, or HPC-1s. Representative cell cycle analysis of murine CD48^{-}CD150^{+}LSK cells (LT-HSCs) by BrdU staining (left). Summary of BrdU uptake in LT-HSCs, MPPs and HPC-1s quantified in the graphs (right) (n=5 mice per group). **H**, CHD7 deficiency does not affect quiescence of LT-HSCs, MPPs or HPC-1s. Representative intracellular Ki-67 and DAPI staining of LT-HSCs (left). Quantification of the quiescence data is in the graphs on the right (n=5 mice per group). **I.** CHD7 deficiency does not affect apoptosis of LT-HSCs, MPPs or HPC-1s. Representative Annexin V staining of HPC-1s (left). Quantification of the apoptosis data is in the graph on the right (n = 6-7 mice per group).

J, Percentage of LT-HSCs and HPC-1s in CHD7 deficient bone marrow 7 days following 5-FU treatment (150 mg/kg).

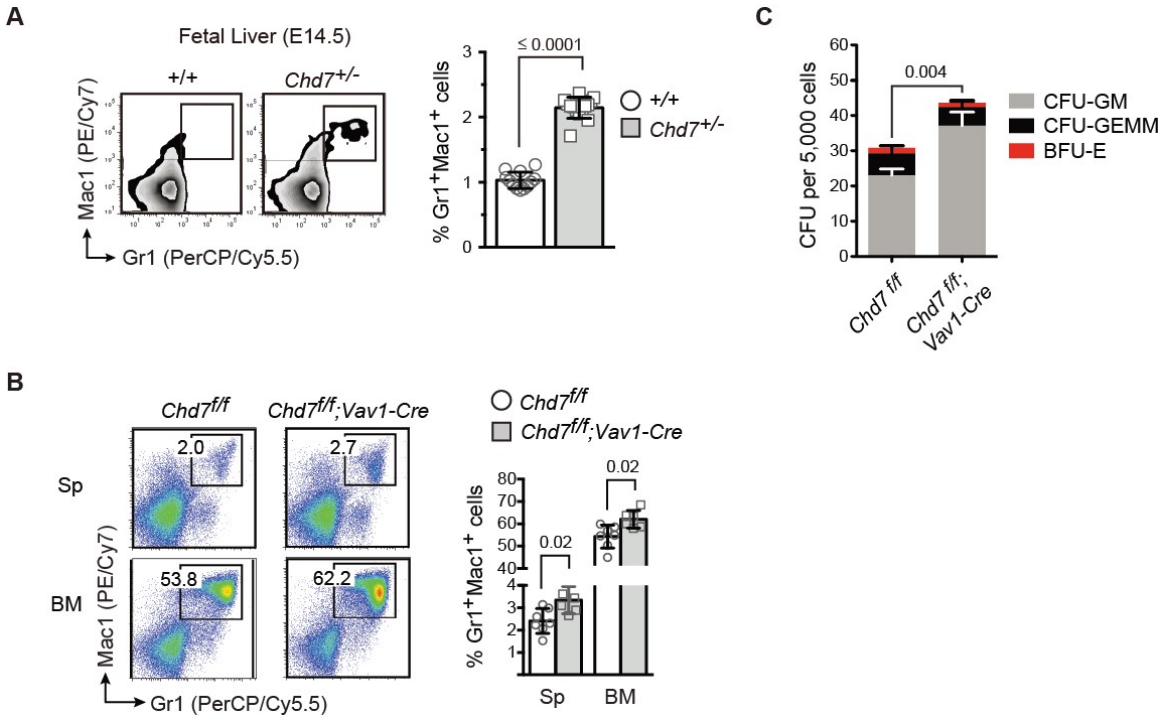
A
Fetal Liver (E14.5)
+/+
Chd7+/-
Mac1 (PE/Cy7)
Gr1 (PerCP/Cy5.5)
% Gr1+Mac1+ cells
≤ 0.0001
+/+
Chd7+/-
C
CFU per 5,000 cells
0.004
CFU-GM
CFU-GEMM
BFU-E
Chd7 f/f
Chd7 f/f; Vav1-Cre
B
Chd7f/f
Chd7f/f;Vav1-Cre
Sp
BM
2.0
2.7
53.8
62.2
0.02
0.02

Figure S4. CHD7 constrains myeloid differentiation. **A**, Increased $Gr1^{+}Mac1^{+}$ cells in fetal livers of *Chd7*$^{+/-}$ embryos by flow cytometry (left), quantified in graph (right) (n=11-15 embryos per group). **B**, *Chd7*$^{f/f}$*;Vav1-Cre* mice have increased $Gr1^{+}Mac1^{+}$ cells in BM and spleen (Sp) by flow cytometry (left), quantified in graph (right) (n=7-9 mice per group). **C**, Increased CFUGM in *Chd7*$^{f/f}$*;Vav1-Cre* BM (n=5 mice per group). CFU, colony forming units, 5 embryos per genotype, n=2 experiments.

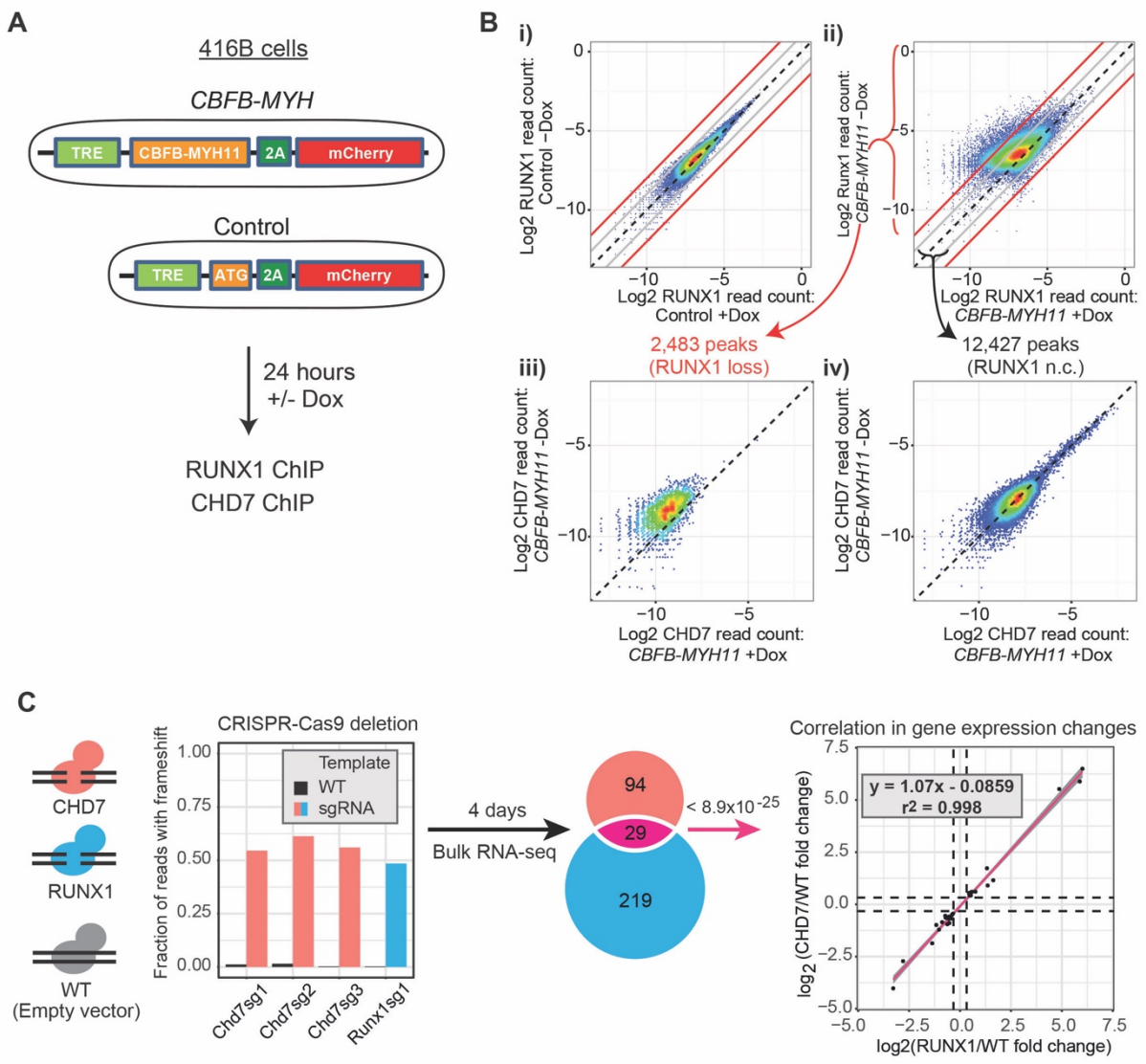
A
416B cells
CBFB-MYH
TRE
CBFB-MYH11
2A
mCherry
Control
TRE
ATG
2A
mCherry
24 hours
+/- Dox
RUNX1 ChIP
CHD7 ChIP
B
i)
Log2 RUNX1 read count: Control −Dox
Log2 RUNX1 read count: Control +Dox
ii)
Log2 Runx1 read count: CBFB-MYH11 −Dox
Log2 RUNX1 read count: CBFB-MYH11 +Dox
2,483 peaks (RUNX1 loss)
12,427 peaks (RUNX1 n.c.)
iii)
Log2 CHD7 read count: CBFB-MYH11 -Dox
Log2 CHD7 read count: CBFB-MYH11 +Dox
iv)
Log2 CHD7 read count: CBFB-MYH11 -Dox
Log2 CHD7 read count: CBFB-MYH11 +Dox
C
CHD7
RUNX1
WT (Empty vector)
CRISPR-Cas9 deletion
Fraction of reads with frameshift
Template
WT
sgRNA
Chd7sg1
Chd7sg2
Chd7sg3
Runx1sg1
4 days
Bulk RNA-seq
94
29
219
< 8.9x10-25
Correlation in gene expression changes
y = 1.07x - 0.0859
r2 = 0.998
log2 (CHD7/WT fold change)
log2(RUNX1/WT fold change)

Figure S5. Genomic localization of CHD7 overlaps with active chromatin regions and is selectively lost from RUNX1 binding sites. **A**, Schematic of Tet inducible Control and *CBFBMYH11* constructs transduced into 416B cells. Individual clones were cultured with or without doxycycline for 24 hours. Cells were subsequently collected for ChIP with RUNX1 and CHD7. **B**, Replicate of experiment shown in Figure 3F. RUNX1 occupancy in i) control clone and ii) *CBFB-MYH11* expressing clone. CHD7 occupancy loss is iii) higher in regions of >4-fold RUNX1 occupancy loss and iv) minimally changed in regions of <2-fold RUNX1 occupancy loss. Black dotted line, no change (n.c.). Grey line, 2-fold change. Red line, 4-fold change. **C**, Genes that are differentially expressed in CHD7 and RUNX1 CRISPR/Cas9 knockout cells are tightly correlated. Targeting sgRNAs for CHD7 (n=3) and RUNX1 (n=1) were validated by sequencing to cause 50-60% frameshift mutations compared to empty vector control, and genes differentially expressed in CHD7 knockouts were selected based on expression changes that were shared in a minimum of two out of three sgRNAs (FDR 0.25). Significance of overlapping genes between CHD7 and RUNX1 determined by hypergeometric testing.

Table S1. RUNX1-CBFβ interacting proteins identified by mass spectrometry

IPI Accession number	Description	Total Peptides
IPI00131214.4	RUNT RELATED TRANSCRIPTION FACTOR 1	22
IPI00121608	B-CELL LEUKEMIA/LYMPHOMA 11B	16
IPI:IPI00345676.5	CHROMODOMAIN HELICASE DNA BINDING PROTEIN 7	9
IPI00131148.2	RUNT RELATED TRANSCRIPTION FACTOR 3	7
IPI00120529.2	RECC1 PROTEIN	6
IPI00118921.2	TCF7 TRANSCRIPTION FACTOR 7, T CELL SPECIFIC	5
IPI00116926.3	ZINC FINGER PROTEIN 281	4
IPI00122696.4	HISTONE-BINDING PROTEIN RBBP4	4
IPI00230542.1	ISOFORM B OF FORKHEAD BOX PROTEIN P1	4
IPI00129577.1	AIFM1, APOPTOSIS-INDUCING FACTOR 1, MITOCHONDRIAL	3
IPI00117063.1	RNA-BINDING PROTEIN FUS	3
IPI00119618.1	CALNEXIN	3
IPI00122168.3	TYROSINE-PROTEIN PHOSPHATASE NON-RECEPTOR TYPE 14	3
IPI00122615.2	PML PROTEIN	3
IPI00125457.5	SET DOMAIN CONTAINING 1A	3
IPI00128230.1	METASTASIS-ASSOCIATED PROTEIN MTA2	3
IPI00130591.2	INTERLEUKIN ENHANCER-BINDING FACTOR 3	3
IPI00132762.1	HEAT SHOCK PROTEIN 75 KDA, MITOCHONDRIAL	3
:IPI00229475.1	JUNCTION PLAKOGLOBIN	3
IPI00229784.2	TRANSCRIPTIONAL REPRESSOR P66 ALPHA	3
IPI00230351.1	SUCCINATE DEHYDROGENASE [UBIQUINONE] FLAVOPROTEIN SUBUNIT,MITOCHONDRIAL PRECURSOR	3
IPI00270061.4	12 DAYS EMBRYO SPINAL GANGLION CDNA, RIKEN FULL-LENGTH ENRICHED LIBRARY, CLONE:D130074N24 PRODUCT:SIMILAR TO S164 PROTEIN HOMOLOG (FRAGMENT).	3
IPI00320241.1	DNAJ HOMOLOG SUBFAMILY B MEMBER 11 PRECURSOR	3
IPI00331523.2	LINGERER PROTEIN-2B	3

Supplementary Datasets

Dataset S1. Microarray results for genes up- and down-regulated in *Chd7$^{f/f}$;Vav1-Cre* LT-HSCs.

Dataset S2. Ingenuity Pathway Analysis summary of functions associated with up-regulated genes in *Chd7$^{f/f}$;Vav1-Cre* LT-HSCs.

Dataset S3. CHD7 enriched binding regions in 416B HPCs.

Dataset S4. CHD7 binding from regions of >4 fold RUNX1 binding loss in CBFB-MYH11 expressing HPC cells.

Dataset S5. Differential gene expression analysis of CHD7 and RUNX1 CRISPR/Cas9 knockout 416B cells.